Heavy cosmic rays at sea level

P. C. M. Yock
Physics Department, University of Auckland, Auckland, New Zealand
(Received 30 September 1985; revised manuscript received 13 March 1986)

An experimental study of heavy cosmic rays at sea level has been carried out. Fluxes of protons, deuterons, tritons, and ^{3}He nuclei in various speed intervals between $0.4c$ and $0.6c$ were measured and an upper limit obtained for the α-particle flux. These are reported and compared with earlier measurements. A model is given to account for the fluxes. Four anomalous events were recorded which are difficult to account for in terms of known nuclei. The data are consistent with a flux, of primary origin, of approximately 2×10^{-9} cm^{-2}sec^{-1}sr^{-1} at the zenith of singly charged long-lived particles with mass $\gtrsim 4.5m_p$ but they do not require such a flux. Some theoretical speculations based on the possible existence of heavy particles are briefly given.

I. INTRODUCTION

This paper describes an experimental study of heavy cosmic rays at sea level. Isotopes of hydrogen and helium nuclei in various speed intervals between $0.4c$ and $0.6c$ were observed and their fluxes measured. In the course of the experiment a few anomalous events were recorded which are difficult to account for in terms of known nuclei. The paper reports the measured fluxes for hydrogen and helium and also the characteristics of the anomalous events.

The plan of the paper is as follows. Section II deals with the experiment. The observed fluxes of hydrogen and helium isotopes are given in Sec. III and compared with previous measurements. Also, a model is given to account for the fluxes. The anomalous events are discussed in Sec. IV and some theoretical speculations on possible new particles are also given there. Conclusions are given in Sec. V.

II. EXPERIMENT

The experimental arrangement is shown in Figs. 1 and 2. It comprised a range telescope and it was located at sea level under a roof of a few g/cm^2 thickness. Its operation was similar to that followed in previous work using similar equipment.[1,2] The previous experiment was not able to satisfactorily resolve tritons from deuterons or heavier particles which may be present and this experiment was carried out with improved apparatus in an effort to resolve these particles and to measure fluxes in the $Z=2$ region. The results obtained here on the fluxes of hydrogen and helium isotopes differ in some respects from those reported by other groups.[3–5] For this reason, and because of the presence of the anomalous events mentioned above, experimental details are given.

As in the earlier work[1,2] speeds of particles were obtained from time-of-flight measurements over the path length of the telescope. Pulse heights above the absorber, together with the speed measurements, were used to determine charges of particles. Pulse heights below the absorber were used to determine masses of particles, with

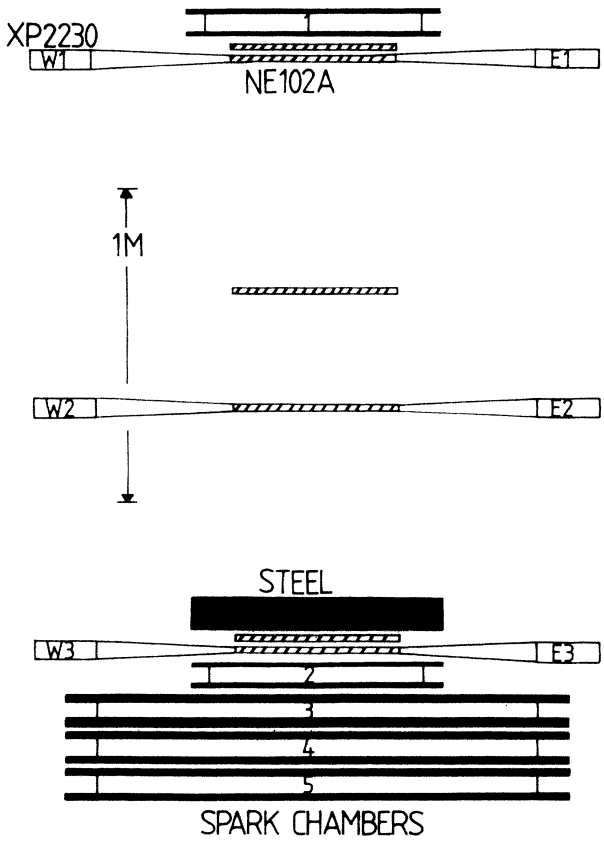

FIG. 1. The range telescope used in the present work. The first, third, and fifth scintillators were viewed by pairs of photomultipliers in the orthogonal (north-south) direction. The thickness of the steel absorber was adjustable between 18.97±0.04 and 76.51±0.08 g/cm^2. The gap between it and the scintillator immediately beneath it was approximately 2 mm wide. The depths of material below the bottom scintillator of the gaps (all 46 mm) of spark chambers Nos. 2, 3, 4, and 5 were respectively 1.6, 6.0, 13.7, and 21.4 g/cm^2 Fe equivalent. The thickness of each scintillator, including wrapping, was 1.02±0.03 g/cm^2 Fe equivalent.

 ©1986 The American Physical Society

FIG. 2. The scintillators and adiabatic light guides (supplied by Carville Ltd., Surrey) of the telescope. The scintillator dimensions are $504\times504\times6$ mm^3. Each scintillator was mapped using a small ^{90}Sr source as a source of localized (β) radiation. The light transit times of the fingers of the guides were found to be uniform to better than $\pm$ 100 psec and their relative light transmission factors uniform to better than $\pm7\%$. The photomultipliers were cemented to the light guides.

heavier particles producing smaller pulses according to the equation

$$\frac{m}{m_p}=\frac{q^2T}{R(\beta)-R(\beta')}\,. \tag{1}$$

Here m_p denotes the proton mass, T the thickness of the main absorber (corrected for the finite thicknesses of the scintillators), q denotes charge, β and β' the speeds above and below the absorber, and R the range in steel of a proton. The function R has been tabulated by Janni.[6] The speed β' was determined from the pulse heights in the bottom scintillators.

The method is analogous to conventional mass spectroscopy with the absorber replacing the magnetic field. Adjustments of the magnetic field strength were mimicked by changing the thickness of the absorber, which was in the form of thin sheets. The technique enjoys the advantages of ease of operation over large areas and solid angles and for long times—important considerations for some cosmic-ray experiments. On the other hand, there is the obvious complication brought about by nuclear interactions sometimes occurring in the absorber. When interactions occur Eq. (1) does not apply of course.

In this experiment nuclear interactions were recognized in two ways. The spark chambers were operated in the track following mode and photographed stereoscopically to observe scattering. Also the penetration into the bottom section of the telescope and the pattern of pulse heights in the scintillators were used to identify inelastic nuclear interactions (see later).

The range technique requires for its utilization that an observable decrease in speed occur in the absorber. This was achieved here by employing a time-of-flight trigger to select particles with speeds $\lesssim0.65c$. The slow particle trigger was fivefold ($E_1E_3\widetilde{W}_1W_3W_2$) and utilized constant fraction discriminators.[7] Its efficiency is noted below.

For triggered events all twelve photomultiplier outputs were displayed on two fast oscilloscopes (modified[8] Hewlett-Packard 183A's) and photographed. Timing and pulse-height measurements were made directly from these photographs.

Time-of-flight measurements were calibrated in regularly held muon runs, involving a total of approximately 900 muons, using a normal twofold trigger (E_1W_3) at half the muon pulse height. Spark-chamber trajectories were used to select single-muon events. The zenith angle effect on path length and light transit times in the scintillators (measured speed $\approx0.50c$) were taken into account for each event. A sample of muon pulses is shown in Fig. 3. The time bases of the oscilloscopes were monitored regularly using a crystal controlled oscillator as shown in Fig. 4.

Pulse-height measurements were calibrated in regularly held proton runs, involving a total of approximately 800

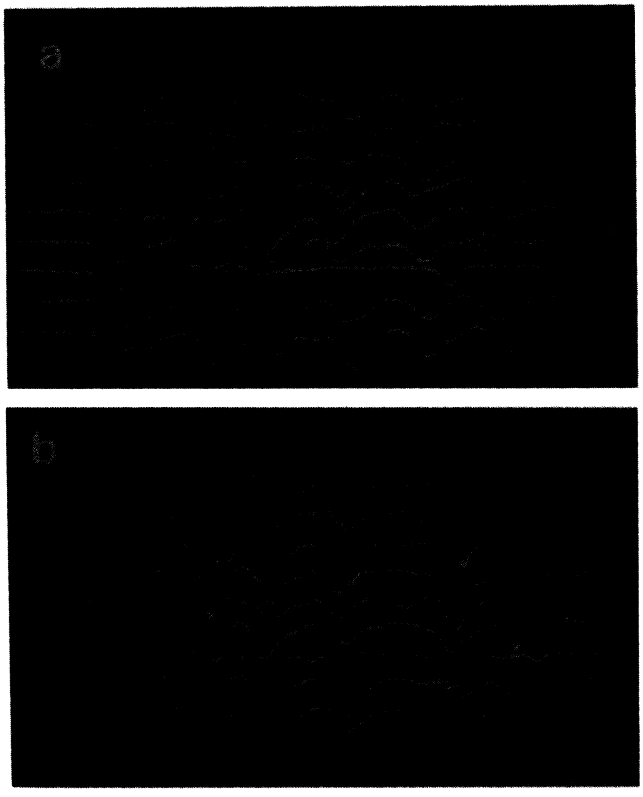

FIG. 3. Typical muon traces used for timing calibrations. (a) shows the east-west photomultiplier pulses for nine events of which eight were clearly muons, and (b) shows the NS pulses for the same events. The orders of the pulses are, respectively, $E_1W_1E_2W_2E_3W_3$ and $N_2N_1N_3S_3S_1S_2$. Timing measurements were made from such photographs using a traveling microscope and the constant fraction technique (50%). The pulses shown are negative, anode pulses. They were clipped with shorted 30-cm cables and matched "tees."

protons, using the slow particle trigger mentioned above at the muon pulse height and an absorber thickness of 18.97 ± 0.04 g/cm^2. This thickness was (easily) sufficient to stop muons with $v \lesssim 0.65c$ but at the same time it allowed protons with $v \gtrsim 0.5c$ to pass through. The speed of each proton was computed[9] with the aid of the muon timing data, and hence[6] also its ionization above and below the absorber. These ionizations were compared with the observed pulse heights to calibrate the latter. In doing this the zenith angle, light absorption in the scintillators (measured attenuation length ≈ 80 cm), and the nonlinear light output of scintillators[10] were taken into account for each event. Figure 5 shows the speed spectrum of all single particles observed in the proton runs, and also the efficiency of the slow particle trigger as a function of speed. With the above absorber thickness the trigger rate was several/hour and most triggers were caused by protons. A sample of proton pulses is shown in Fig. 6. The vertical amplifiers of the oscilloscopes were monitored regularly using a constant-pulse-height generator in a similar fashion to that described above to monitor the time bases.

The proton data were used to assess the accuracies of the timing and pulse-height measurements. The EW and NS photomultipliers gave independent time-of-flight measurements for each particle.[11] It was found that the agreement between the two measurements corresponded to a statistical error of 210 psec for the average. The positions of the four midway timing pulses (N_2, E_2, W_2, and S_2) were found to be constrained by the positions of the top and bottom pulses to accuracies of 410 psec and sufficed for selecting single-particle events as reliably as the spark-chamber data. The correlation between the spark-chamber trajectories and tracks determined from timing measurements was found to be ± 3.5 cm (one standard deviation; x and y coordinates) in each of the top, middle, and bottom planes. The correlation between spark-chamber trajectories and tracks determined from pulse-height measurements with light attenuation taken into account was found to be ± 9 cm above the absorber and ± 7 cm below. The pulse-height calibration procedure mentioned above was used to determine the accuracy of the ionization measurements. The average measured ionization in the top four scintillators was found to have a one standard derivation accuracy of approximately 7–8 % at $dE/dx \sim 4.5$ MeV g^{-1}cm^2 and the average in the bottom two scintillators had a similar uncertainty at ~ 7 MeV g^{-1}cm^2. Similar conclusions were reached by com-

FIG. 4. Typical 50-MHz crystal-oscillator traces used to monitor the oscilloscope time bases. The muon trigger (with the spark chambers firing) was used for the oscillator runs. (a) shows the display of the EW oscilloscope and (b) the display of the NS oscilloscope. The time bases of the oscilloscopes were approximately 11 and 13 nsec/division, respectively. The speeds of 920 single sweeps were measured with a traveling microscope from photographs taken through the course of the experiment.

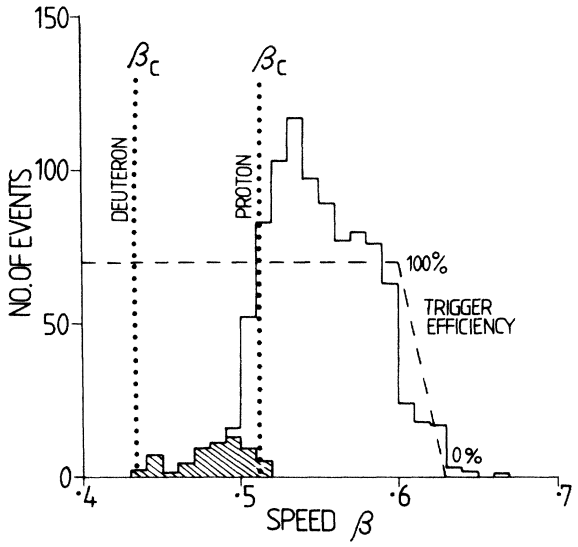

FIG. 5. Speed spectrum of all particles observed in proton calibration runs. The sloping cutoff at $\beta \sim 0.62$ shows the effect of the delayed coincidence trigger. The dashed line giving the trigger efficiency is approximate only. The cutoff at $\beta \approx 0.51$ shows the effect of the (reduced) absorber. Only particles which penetrated at least as far as spark chamber No. 2 were included and the dotted lines are the calculated (Ref. 6) minimum speeds for protons and deuterons to penetrate this far. The shaded events below $\beta = 0.52$ were unambiguously identified as deuterons from their ranges in the spark-chamber stack. For $\beta > 0.52$ the distinction between protons and deuterons was not always unambiguous. In calibrating the pulse-height response of the bottom two scintillators only those protons or deuterons which exhibited the correct range in the spark-chamber stack for the measured time of flight were included.

paring the observed pulse heights produced by individual protons in different scintillator planes. Clearly significant uncertainties in the ionization measurements arose through the use of thin scintillators.[12] The estimated number of photoelectrons per scintillator per muon was 30.

Systematic timing and ionization errors are expected to have been small because of the directness of the oscilloscope technique. They are furthermore expected to have had negligible (i.e., $\ll$ statistical) effects on the mass measurements because they affect the heavy-particle and proton calibration data almost equally. The locations of the deuteron and triton peaks in Fig. 7 (see later) support this.

Drifts are a source of error in a long-term experiment such as this. The analysis that was used neglected drifts in the electronics which occurred in one-month periods. Allowances for drifts were made only monthly. The voltages and gains of the photomultipliers and the time bases and vertical gains of the oscilloscopes were monitored regularly, and it was anticipated that errors due to drifts that occurred in any month would be considerably smaller than statistical effects. Subsequent analysis of the muon and proton calibration data indicated that timing drifts which occurred in the course of the experiment were

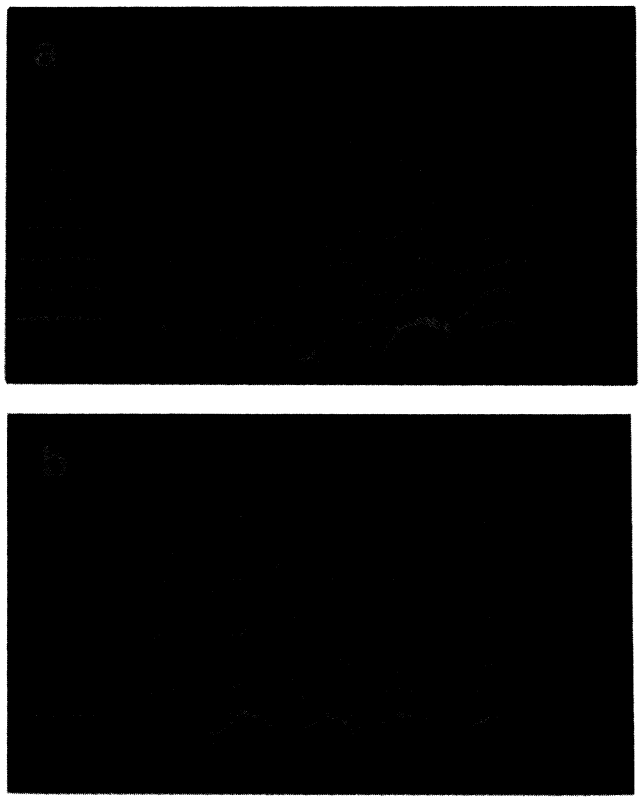

FIG. 6. Typical proton traces used for pulse-height calibrations. (a) shows the EW pulses and (b) the NS pulses for the same events. The gains of the oscilloscopes were reduced by a factor of 2 relative to that used in the muon runs. The slower speeds and higher ionizations of the protons relative to the muons are apparent.

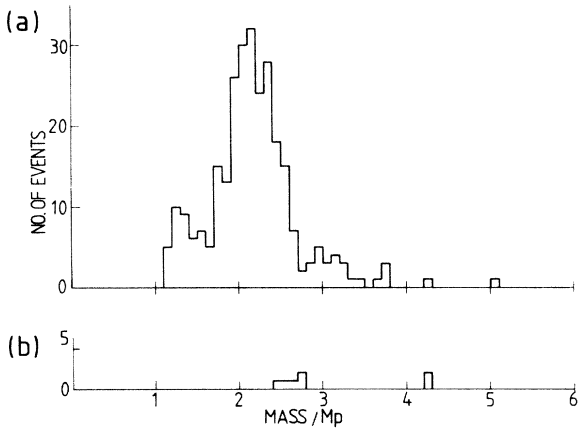

FIG. 7. Measured mass spectrum of particles detected in the charge-one run. (a) is the spectrum for events in which the increase in ionization in traversing the absorber was greater than 20%. (b) is the spectrum of lower limits at a calculated 90% confidence level for events in which the increase was less than 20%.

<50 psec and thus negligible, and that, after the first two months of operation, the photomultiplier gains decreased smoothly, typically at a rate of 9% per annum, and thus negligibly in any one month period. In order to minimize drifts the equipment was maintained at constant temperature and the main ac supply was regulated. Also, the photomultipliers were run at fairly low voltages, typically 2100 V.

III. FLUXES OF HYDROGEN AND HELIUM

Two runs, each of approximately 5000 h effective duration, were held. The first was sensitive to deuterons and tritons and the second to ^{3}He nuclei and α particles.

For deuterons and tritons an absorber thickness of 66.90 ± 0.08 g/cm^2 was used for 2000 h and 76.51 ± 0.08 g/cm^2 for 3000 h. The slow particle trigger described in the previous section was used at the muon pulse height. Results obtained are shown in Figs. 7 and 8. All single-particle events with speed $<0.65c$ are shown. Equation (1) with q set equal to unity was used to calculate particle masses. Speeds below the absorber were determined from the pulse heights in the bottom two scintillators assuming a charge of unity. The photomultiplier pulses for a typical five-hour run are shown in Fig. 9. The single-particle events generally showed up from a glance at the oscilloscope photographs.

Figure 7(a) includes all events for which the increase in ionization in traversing the absorber was greater than 20%. For these events Eq. (1) predicts a measurement accuracy which varies from event to event but is typically $^{+0.25}_{-0.20}m_p$ for deuterons and $^{+0.50}_{-0.40}m_p$ for tritons. These accuracies were calculated from the proton calibration data given in Sec. II. The seven events shown in Fig. 7(b) exhibited an increase in ionization of less than 20% and for these events the uncertainty in mass is greater. Here lower limits on the mass at a calculated 90% confidence level are given only.

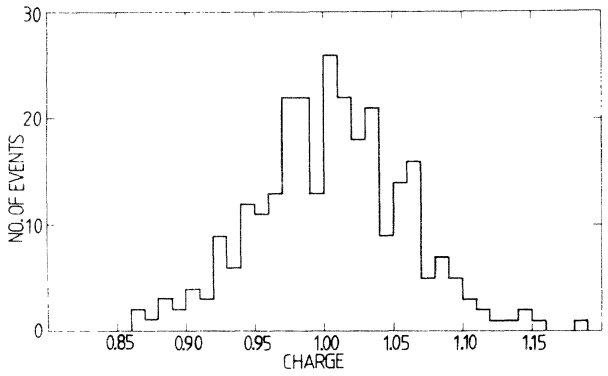

FIG. 8. Measured charge spectrum of particles detected in the charge-one run. The expected accuracy of the measurements, as determined from the proton calibration data, is ± 0.05. Seven events with anomalously large pulses in scintillators above the absorber, which obviously resulted from interactions, are not included.

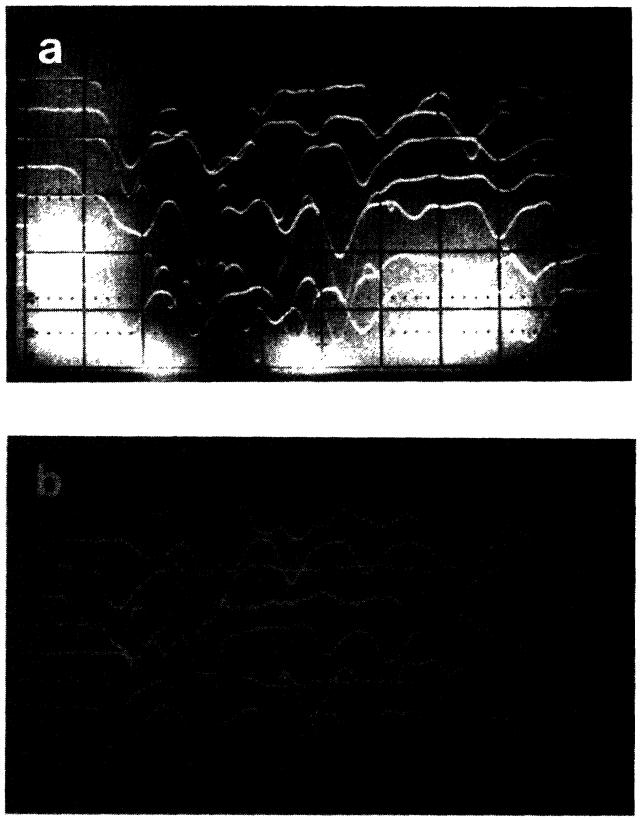

FIG. 9. Typical photomultiplier traces obtained in a five-hour run during the course of the experiment. (a) shows the EW pulses for eight triggers and (b) the NS pulses for the same events. Only the last event was a single-particle event. The charge and mass for this event, as calculated from the measured pulse heights and spacings, are $\pm 1.01e$ and $2.08 m_p$, respectively; clearly a deuteron. Its measured speed was $0.578c$ and it reached the third spark chamber.

All but the two heaviest events in Fig. 7(a) are consistent with deuteron or triton identifications except for some protons, which just satisfied the delayed coincidence trigger, on the tail of a distribution. The five lighter events of Fig. 7(b) are consistent with triton identifications. The four remaining particles, two on Fig. 7(a) and two on Fig. 7(b), appear to be heavier than tritons. Further discussion of these anomalous events is given in the following section. For the events on Fig. 7(a) at approximately $3.6 m_p$ identifications in terms of either tritons or heavier particles are consistent. The same also applies to the five lighter events on Fig. 7(b) of course.

For helium nuclei an absorber thickness of 18.97 ± 0.04 g/cm^2 was used with the slow particle trigger and discrimination levels of approximately three times the muon pulse height. This resulted in a trigger rate of about six per day. The gains of the oscilloscopes were of course reduced to accommodate the larger pulses in this mode of operation.

The results from 5000 h of effective operation are given in Table I. They indicate that, during this two-year run, the telescope functioned in accordance with the accuracies determined by the proton calibration data. No evidence for anomalous doubly charged particles was obtained. The ^{3}He nuclei detected in this run showed up particularly clearly in the oscilloscope photographs because of the large pulse heights.

Fluxes of hydrogen and helium nuclei may be calculated from the data presented in Figs. 5 and 7 and Table I. Fluxes so obtained, allowing for loss of events due to interactions occurring in the absorber (assumed absorption length 100 g/cm^2) are given in Table II. For purpose of comparison, data from other experiments have been included.

The reported fluxes for protons and deuterons in the table appear to be compatible as far as the differing conditions of the measurements allow comparison.

Deuterons and tritons with speeds $\sim 0.5c$ are produced copiously in medium-energy interactions. Kamal *et al.*[13] reported the observation of one deuteron with $0.41 < \beta < 0.77$ per 14 stars in an exposure of nuclear emulsion to 24 GeV/c protons and a similar rate in a pion exposure. The deuterons were not confined to small angles. If we assume that at low altitudes most slow deuterons, tritons, and ^{3}He nuclei are produced as secondaries in such interactions, then ratios of their fluxes may be calculated. Schwarzschild and Zupančič[14] reported a d:t yield ratio ≈ 20 and Gilly *et al.*[15] a t:^{3}He yield ratio ≈ 1 in accelerator experiments. These figures imply d:t and t:^{3}He flux ratios of approximately 14 and 4, respectively, in any speed interval.[16] The absolute flux of deuterons with $v \sim 0.5c$ would be expected to be an order of magnitude less than the proton flux[17] above a few GeV, i.e., $\sim 10^{-6}$ cm^{-2}sec^{-1}sr^{-1} at sea level. The deuterons would not be limited to small angles about the zenith.

The above expectations are in reasonable agreement with the results of the present experiment. The triton flux reported in Ref. 3 appears to be relatively high and this suggests that the sample of particles identified therein as tritons included other types of particles. The nonobservation of any ^{3}He in that experiment further supports this

TABLE I. Data for all events recorded in the charge-two run. The uncertainties for the charge and mass measurements were calculated from the proton calibration data. A systematic error in the charge measurements is evident. Events 1573/1 and 1683/1 clearly involved fragmentation in the absorber with protons reaching the bottom two scintillators. Mass measurements are not possible in such events. For the other events masses were determined from Eq. (1) with q set equal to two.

Event No.	Speed β ± 0.011	$\lvert$Charge$\rvert$ ± 0.07	Mass/m_p ± 0.4	Identification
1498/5	0.589	2.14	2.41	^{3}He
1532/1	0.552	2.03	3.04	^{3}He
1556/1	0.558	2.01	2.66	^{3}He
1560/4	0.567	2.00	3.72	^{3}He or α
1573/1	0.518	2.01		^{3}He?
1683/1	0.543	2.06		^{3}He?
1757/2	0.559	2.18	2.48	^{3}He
1763/4	0.573	2.04	3.33	^{3}He
1826/9	0.551	2.06	2.97	^{3}He

conclusion. Based on a sample of 23 events the authors of Ref. 5 reported a sea-level deuteron flux $\sim 10^{-8}$ cm^{-2}sec^{-1}sr^{-1} with $0.5 < \beta < 0.6$ at large zenith angles. This is too low to be accommodated in the above framework.

IV. HEAVY PARTICLES

The data for the four anomalous events recorded in the 5000-h $Z = 1$ run are given in Table III. The photomultiplier pulses for event 386/6 are shown in Fig. 10.

The errors and confidence levels given in the table were calculated from Eq. (1) assuming accuracies for the timing and pulse-height measurements as determined in the proton calibration runs (Sec. II). The same method was used to predict the accuracies of the measurements, as quoted in the preceding section, for deuterons, tritons, and helium nuclei. The observed distributions of deuterons shown in Figs. 7 and 8 are consistent with the expectations. Also, the observed distributions for helium isotopes given in Table I are consistent with the expectations. For tritons, however, the observed distributions appear to be consistent only if most of the anomalous events were not tritons. This suggest an explanation for these events in terms of particles other than tritons.

The possibility that the anomalous events were multiparticle events with measured charges consistent, by chance, with unity seems unlikely. In the earlier work of Ref. 2 there was considerably less information per event.

TABLE II. Fluxes of hydrogen and helium isotopes as determined in this experiment. Data from other experiments are included for purpose of comparison. Not included in the mountain-altitude data from Ref. 4 is a relatively high α-particle flux reported therein. Later runs failed to confirm this flux. The author thanks Professor T. Bowen for informing him of this.

Species	Speed interval β	Number observed	Flux (cm^{-2}sec^{-1}sr^{-1})
Sea-level data from this experiment			
p	0.51—0.615	780±20	$1.4\pm0.2\times10^{-5}$
d	0.435—0.52	61	$8.5\pm1.3\times10^{-7}$
d	0.57—0.615	218±10	$1.4\pm0.2\times10^{-7}$
t	0.52—0.615	25±5	$1.6\pm0.5\times10^{-8}$
^{3}He	0.545—0.615	6 or 7	$2.8\pm1.1\times10^{-9}$
α	0.51—0.615	1 or 0	$<1.3\times10^{-9}$
Sea-level data from Ref. 3			
p	0.63—0.72	≈ 70	$1.8\pm0.3\times10^{-5}$
d	0.55—0.70	≈ 30	$2.3\pm0.6\times10^{-7}$
t	0.57—0.7	16	$8.8\pm2.4\times10^{-8}$
Mountain-altitude (2750 m) data from Ref. 4			
p	0.5—0.6	646	$1.8\pm0.3\times10^{-4}$
d	0.35—0.5	10	$7.3\pm2.8\times10^{-6}$
d	0.5—0.6	8	$5.2\pm2.1\times10^{-6}$
t	0.35—0.7	≤ 2	$\leq 3.2\times10^{-6}$
^{3}He	0.35—0.7	≤ 2	$\leq 3.2\times10^{-6}$

TABLE III. Data for the four anomalous events recorded in the charge-one run. For the first two events lower limits for the masses at a calculated 90% confidence level only are given, as explained in the text.

Event no.	Speed β ± 0.011	|Charge| ± 0.05	Mass/m_p
40/5	0.624	1.00	>4.29
386/6	0.536	0.98	>4.26
550/5	0.543	1.07	$5.05^{+1.0}_{-0.7}$
842/1	0.549	0.98	$4.22^{+0.7}_{-0.6}$

A few events, all having extra sparks in the spark chambers, were observed and reported which could be interpreted as accompanied, fractionally charged, heavy particles. In the present work one such event was observed which satisfied, barely, the extra necessary constraints. The sparks were of poor quality and one of the twelve photomultiplier pulses was poorly shaped. It is assumed here that this event and also the former events were ordinary multiparticle events only. The raw data for the anomalous events listed in Table III are not suggestive of a multiparticle interpretation and in view of the degree of redundancy of information per event it is assumed here that they were single-particle events.

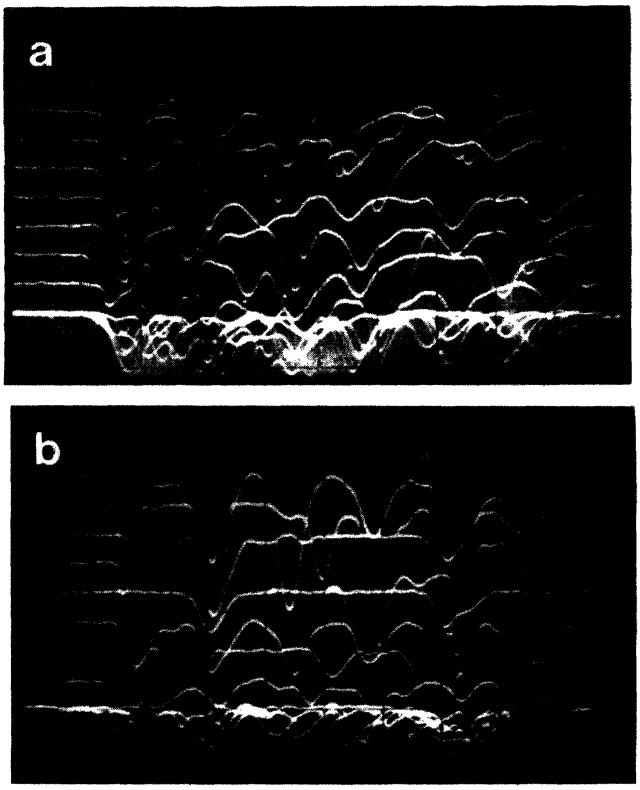

FIG. 10. Photomultiplier pulses recorded in a 14-h run during the experiment. (a) shows the EW pulses for several triggers and (b) the NS pulses for the same events. The sixth event appears to be a single particle event. This is one of the anomalous events, No. 386/6.

Single-particle events can, in exceptional circumstances, produce erroneously high-mass measurements when interactions occur in the absorber. If a proton is incident on the telescope, it may interact near the top of the main absorber to produce a neutron which may in turn interact near the bottom of the absorber to produce a low-energy proton and large signals in both bottom scintillators. In such cases the timing requirements for single-particle events are satisfied and Eq. (1) may yield anomalously high-mass values. The low-energy protons in these events have very short ranges and they were eliminated here by accepting for analysis only those particles which fired spark chamber No. 2. All four anomalous events in Table III fired all the spark chambers in the telescope.

A similar charge-exchange process may account for the anomalous events but the probability appears low. If a deuteron is incident and strips near the top of the main absorber on the periphery of a nucleus it may produce a neutron moving with approximately the same speed and direction. The neutron yield per deuteron is[18] approximately 10^{-2}. If the neutron subsequently undergoes charge exchange with a proton on the periphery of a nucleus near the bottom of the absorber, this may produce a proton still with approximately the same direction and speed. If the total deflection is to be $\lesssim 5°$, as the spark-chamber data require, the proton yield[19] per neutron will be $\lesssim 10^{-4}$. The overall process would appear as a particle with an anomalous range at a flux $\lesssim 10^{-6}$ times the deuteron flux. This is $\lesssim 10^{-3}$ times the observed flux.

Kaons could account for the observations but here again the probability seems low. The medium-energy pion and nucleon fluxes at sea level are known[17] and from these the flux of slow kaons emerging from the roof (7 g/cm^2 thickness) above the telescope may be calculated.[20] The probability that these will decay into fast muons or pions just above the main absorber and in so doing mimic heavy particles penetrating the entire telescope may be calculated. The calculated background rate for this process is $\lesssim 10^{-4}$ times the observed rate. Other processes which have been considered have lower probabilities.

It appears that if the anomalous events in Table III are not examples of heavy particles then they were ^{3}H nuclei for which the ionization and/or timing measurements involved atypically large errors. The argument against this possibility given at the beginning of this section is suggestive but not compelling in the author's opinion.

If new, heavy particles are present, then the observed flux is approximately 2×10^{-9} cm^{-2}sec^{-1}sr^{-1}. This is consistent with the conclusion of Ref. 2 and with all other[3-5,21] experimental studies of slow cosmic rays known to the author. If, on the other hand, the data are used to compute an upper limit only, a flux $<10^{-8}$ cm^{-2}sec^{-1}sr^{-1} is obtained. These fluxes apply to particles with residual ranges at sea level of between 70 and 320 g/cm^2 Fe for a mass of $4.5m_p$ and to greater maximum ranges for heavier particles.

Accelerator searches for long-lived particles of a few proton masses yielded a few inconclusive events at $\sim 4.5m_p$ at a pair-production cross section typical of weak interactions.[22] Such a cross section is not accessible in the present experiment and it follows that if heavy par-

ticles are present, then they are not pair produced in the upper atmosphere but are instead of primary origin.

The unconventional hypothesis that a new type of particle might be present in the primary radiation presupposes the existence of sources of cosmic rays other than those usually considered, such as supernovae, since these are expected to emit known particles and nuclei only.

The recent report[23] of antiprotons in the cosmic radiation having energies below those they would have if pair produced lends support to the possible existence of new cosmic ray sources. It has been suggested that the antiprotons are produced by evaporating primordial black holes with Schwarzschild radii $\approx$ the nucleon Compton wavelength.[24] Interestingly, such black holes are predicted to be evaporating just about now.[25]

This evaporation process could conceivably be the source of particles more exotic than antiprotons. If black holes radiate like blackbodies with particle-emission rates depending only on particle masses, spins, and charges[26] and not on internal structure, then they may be an effective source of particles with complex, tightly bound substructures for which the usual pair-production process would have a low probability at threshold. If complex particles with masses $\sim m_p$ exist, then they may be present at levels comparable to the antiproton flux and yet not be prominent in accelerator experiments.

Particles with complex substructures have been hypothesized to exist by several authors,[27] although the binding of the substructure has not always been envisaged to be strong. This is an important consideration for the black-hole evaporation process which is not expected to produce loosely bound objects. In this respect it is noteworthy that in the above quoted antiproton experiment no $\bar{\alpha}$'s were seen.

Black holes may not exhaust the possibilities for new particles of low energy in the cosmic radiation. Such particles may conceivably contribute to the dark matter of galaxies. Specific suggestions along these lines have been made.[28] Reported observations[29] of new phenomena occurring in cosmic-ray interactions of high energy may have related implications for low-energy phenomena. This will be discussed elsewhere.

V. CONCLUSIONS

The fluxes of the isotopes of hydrogen and helium in the low-energy cosmic radiation at sea level have been measured with results as given in Table II. Some discrepancies with previous measurements by other groups are present. The model given in Sec. III may account for the fluxes.

Four events were recorded which are difficult to account for in terms of known nuclei. They are consistent with a flux $\approx 2\times 10^{-9}$ cm^{-2}sec^{-1}sr^{-1} of singly charged long-lived particles with mass $\gtrsim 4.5 m_p$ but a triton identification cannot be ruled out.

If new particles are present, then they would be of primary origin. The flux may be dependent on the geomagnetic latitude,[30] and would be greater at higher altitudes. Black holes are a possible, if speculative, source of new particles in the primary radiation.

The absorber technique used here for mass spectroscopy has advantages for experiments requiring an extensive geometrical aperture but it entails a consideration of background phenomena. The oscilloscope technique for recording photomultiplier pulses, when combined with a selective trigger, allows a selected subset of a large sample of events to be fully analyzed. Similar techniques were used in the Caltech antiproton experiment (Ref. 23) and they may have useful applications elsewhere.

ACKNOWLEDGMENTS

The author acknowledges discussions and/or correspondence with Professor T. Bowen, Professor S. Hasegawa, Professor L. W. Jones, Professor R. F. Keam, and Professor L. Lyons. R. Beishvizen is thanked for assistance with microscopy. The experimental work was carried out with the aid of New Zealand Universities Grants Committee and University of Auckland research grants.

---

[1]C. R. Alcock *et al.*, Nucl. Instrum. Methods **115**, 245 (1974).

[2]P. C. M. Yock, Phys. Rev. D **23**, 1207 (1981).

[3]A. M. Bakich *et al.*, J. Phys. E **11**, 123 (1978); J. Phys. G **5**, 433 (1979); in *Sixteenth International Cosmic Ray Conference, Kyoto, 1979, Conference Papers* (Institute of Cosmic Ray Research, University of Tokyo, Tokyo, 1979), Vol. 6, p. 53.

[4]H. B. Barber *et al.*, Phys. Rev. D **22**, 2667 (1980).

[5]A. Marini *et al.*, Phys. Rev. D **26**, 1777 (1982).

[6]J. F. Janni, U.S. Air Force Report No. AFWL-TR-65-150, 1966 (unpublished).

[7]The trigger required a coincidence of coincidences. Delayed coincidences of E_1E_3 and also W_1W_3 pulses were required. Coincidences of these coincidences with a W_2 pulse were also required. Constant fraction discriminators (Ortec 934) were used for E_1E_3 and W_1W_3 coincidences.

[8]This model oscilloscope, which is no longer produced, was chosen because it has a relatively bright, crisp trace and also good cathode-ray-tube (CRT) geometry. The modifications involved replacement of several fairly critical trimming potentiometers with fixed metal film resistors in an effort to improve the stabilities of the time bases, lowering of the filament currents to the minimum possible levels for fast single-shot photography to extend the CRT lifetimes, and physical isolation of the power transformers from the immediate vicinities of the CRT's to reduce unwanted magnetic deflections of the cathode rays.

[9]The computing was done by Schiff Computer Services, Auckland.

[10]G. D. Badhwar *et al.*, Nucl. Instrum. Methods **57**, 116 (1967).

[11]They were powered by different Fluke 415B supplies and displayed on different oscilloscopes in different orders.

[12]J. M. Paul, Nucl. Instrum. Methods **96**, 51 (1971).

[13]A. A. Kamal *et al.*, Nuovo Cimento **43A**, 91 (1966).

[14]A. Schwarzschild and Č. Zupančič, Phys. Rev. **129**, 854 (1963).

[15]L. Gilly *et al.*, in *Proceedings of the International Conference*

on High Energy Physics, Rochester, 1960, edited by E. C. G. Sudarshan *et al.* (University of Rochester, Rochester, New York, 1960), p. 808.

[16]These flux ratios follow from the yield ratios by including a range factor for each nuclide $\propto$ mass/(charge)^2. Nuclear interactions would tend to reduce the latter flux ratio.

[17]G. Brook and A. W. Wolfendale, Proc. Phys. Soc. London **83**, 871 (1964).

[18]J. R. Oppenheimer, Phys. Rev. **47**, 845 (1945); A. C. Helmholz *et al.*, *ibid.* **72**, 1003 (1947); R. Serber, *ibid.* **72**, 1008 (1947); S. M. Dancoff, *ibid.* **72**, 1017 (1947).

[19]J. Hadley *et al.*, Phys. Rev. **75**, 351 (1949); D. E. Bainum *et al.*, Phys. Rev. Lett. **44**, 1751 (1980).

[20]P. Baumel *et al.*, Phys. Rev. **108**, 1322 (1957).

[21]H. Kasha and R. J. Stefanski, Phys. Rev. **172**, 1297 (1968); P. Franzini and S. Shulman, Phys. Rev. Lett. **21**, 1013 (1968); F. Ashton *et al.*, Phys. Lett. **B29**, 249 (1969); A. M. Galper *et al.*, Yad. Fiz. **2**, 336 (1970) [Sov. J. Nucl. Phys. **10**, 193 (1970)]; in *Proceedings of the Twelfth International Conference on Cosmic Rays, Hobart, 1971,* edited by A. G. Fenton and K. B. Fenton (University of Tasmania Press, Hobart, Tasmania, 1971), Vol. 6, p. 2317.

[22]D. Cutts *et al.*, Phys. Rev. Lett. **41**, 363 (1978); A. Bussiere *et al.*, Nucl. Phys. **B174**, 1 (1980).

[23]Andrew Buffington *et al.*, Astrophys. J. **248**, 1179 (1981); **247**, L105 (1981).

[24]P. Kiraly *et al.*, Nature (London) **293**, 120 (1981); Michael S. Turner, *ibid.* **297**, 379 (1982).

[25]Bernard J. Carr, Astrophys. J. **206**, 8 (1976); Don N. Page, Phys. Rev. D **16**, 2402 (1977).

[26]S. W. Hawking, Phys. Rev. D **14**, 2460 (1976).

[27]Kenju Mori and Hiroshi Nakamura, Prog. Theor. Phys. **54**, 1228 (1975); A. De Rújula *et al.*, Phys. Rev. D **17**, 285 (1978); J. D. Bjorken and L. D. McLerran, *ibid.* **20**, 2353 (1979); P. C. M. Yock, Ann. Phys. (N.Y.) **82**, 449 (1974).

[28]Edward Witten, Phys. Rev. D **30**, 272 (1984); A. De Rújula and S. L. Glashow, Nature (London) **312**, 734 (1984).

[29]C. M. G. Lattes *et al.*, Phys. Rep. C **65**, 151 (1980); T. Dzikowski *et al.*, J. Phys. G **9**, 459 (1983); M. L. Marshak *et al.*, Phys. Rev. Lett. **54**, 2079 (1985); **55**, 1965 (1985); G. Battistoni *et al.*, Phys. Lett. **155B**, 465 (1985); W. Ochs and L. Stodolsky, Phys. Rev. D **33**, 1247 (1986).

[30]This experiment was carried out at Auckland where the geomagnetic cutoff is ~ 4.5 GV/c.

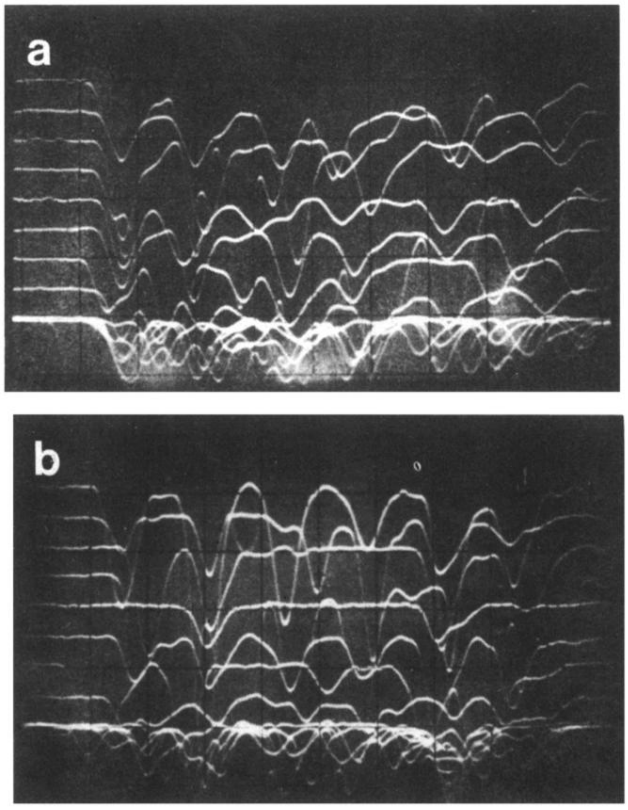

FIG. 10. Photomultiplier pulses recorded in a 14-h run during the experiment. (a) shows the EW pulses for several triggers and (b) the NS pulses for the same events. The sixth event appears to be a single particle event. This is one of the anomalous events, No. 386/6.

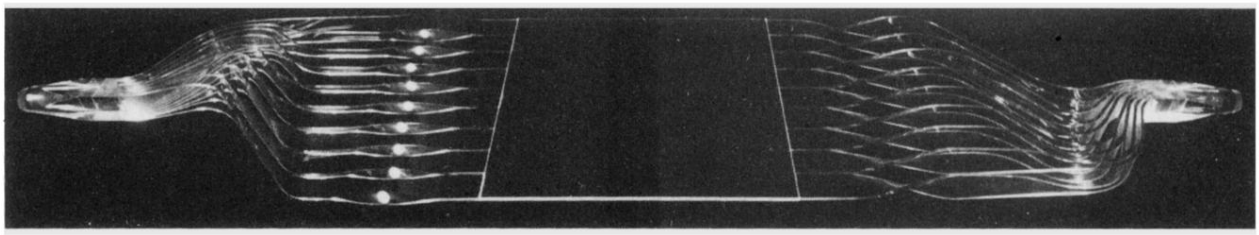

FIG. 2. The scintillators and adiabatic light guides (supplied by Carville Ltd., Surrey) of the telescope. The scintillator dimensions are $504 \times 504 \times 6$ mm^3. Each scintillator was mapped using a small ^{90}Sr source as a source of localized (β) radiation. The light transit times of the fingers of the guides were found to be uniform to better than $\pm$ 100 psec and their relative light transmission factors uniform to better than $\pm 7\%$. The photomultipliers were cemented to the light guides.

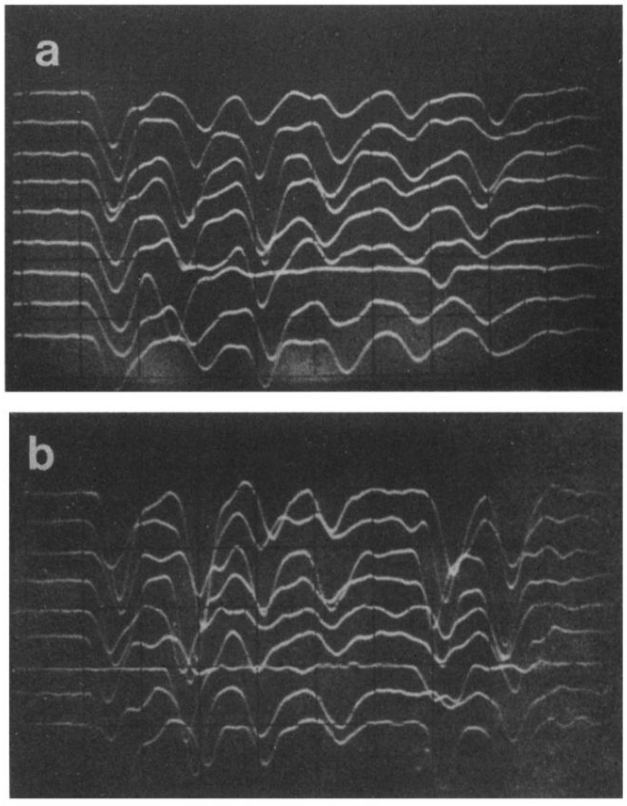

FIG. 3. Typical muon traces used for timing calibrations. (a) shows the east-west photomultiplier pulses for nine events of which eight were clearly muons, and (b) shows the NS pulses for the same events. The orders of the pulses are, respectively, $E_1W_1E_2W_2E_3W_3$ and $N_2N_1N_3S_3S_1S_2$. Timing measurements were made from such photographs using a traveling microscope and the constant fraction technique (50%). The pulses shown are negative, anode pulses. They were clipped with shorted 30-cm cables and matched "tees."

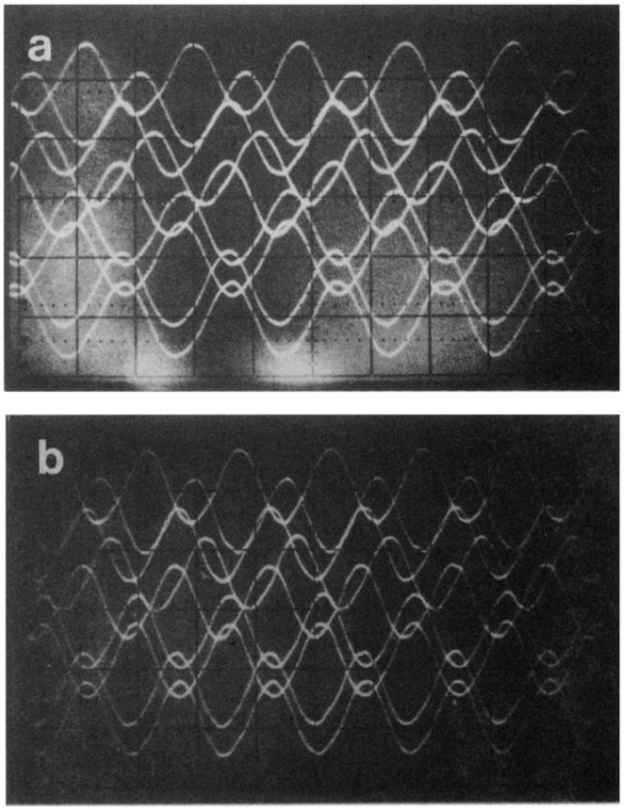

FIG. 4. Typical 50-MHz crystal-oscillator traces used to monitor the oscilloscope time bases. The muon trigger (with the spark chambers firing) was used for the oscillator runs. (a) shows the display of the EW oscilloscope and (b) the display of the NS oscilloscope. The time bases of the oscilloscopes were approximately 11 and 13 nsec/division, respectively. The speeds of 920 single sweeps were measured with a traveling microscope from photographs taken through the course of the experiment.

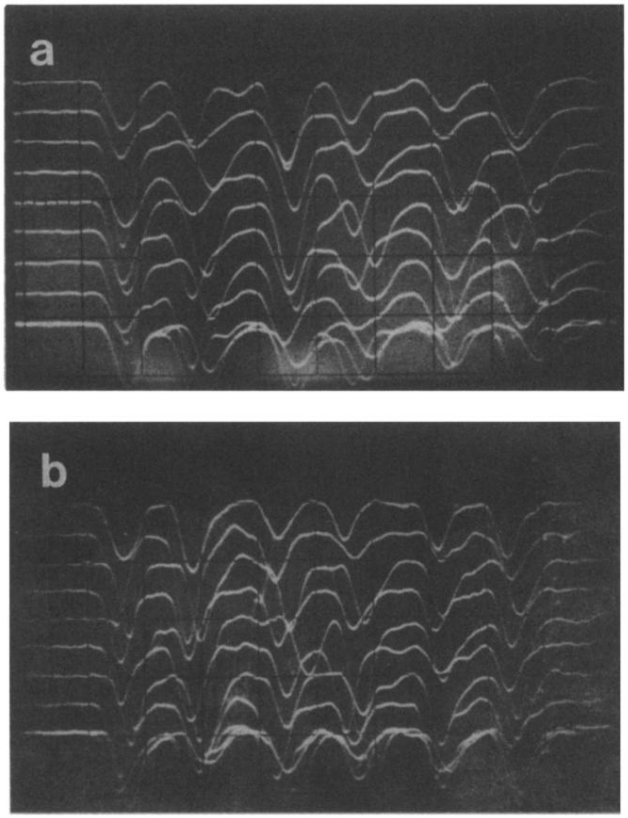

FIG. 6. Typical proton traces used for pulse-height calibrations. (a) shows the EW pulses and (b) the NS pulses for the same events. The gains of the oscilloscopes were reduced by a factor of 2 relative to that used in the muon runs. The slower speeds and higher ionizations of the protons relative to the muons are apparent.

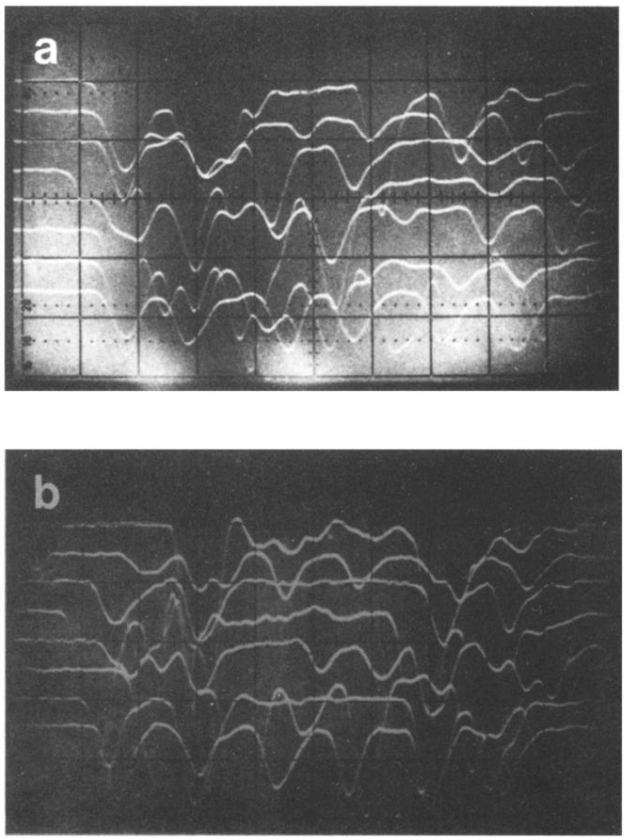

FIG. 9. Typical photomultiplier traces obtained in a five-hour run during the course of the experiment. (a) shows the EW pulses for eight triggers and (b) the NS pulses for the same events. Only the last event was a single-particle event. The charge and mass for this event, as calculated from the measured pulse heights and spacings, are $\pm 1.01e$ and $2.08 m_p$, respectively; clearly a deuteron. Its measured speed was $0.578c$ and it reached the third spark chamber.